

Multiple Sensor Fusion-Based Positioning Robot for Steam Generator Inspection

Jingwei You^{a,b,c}, Shouqi Wei^a, Xiong Wu^{a,b,c}, Jianquan Sun^{*b,c}^a Department of Electrical Engineering, Guilin University of Electronic Technology, Guilin, China 541004;^b Guangdong Provincial Key Lab of Robotics and Intelligent System, Shenzhen Institutes of Advanced Technology, Chinese Academy of Sciences, Shenzhen, China 518000;^c SIAT-CUHK Joint Laboratory of Robotics and Intelligent Systems, Shenzhen, China 518000

* Corresponding author: jq.sun@siat.ac.cn

Abstract: Nuclear energy is presently the clean energy source most likely to massively displace fossil energy, and the secondary side of the steam generator is an important part of a nuclear power plant. Due to the small space of the secondary side of the steam generator and the confinement of the vessel, the precise positioning of the robot inside the steam generator cannot be achieved by a single sensor alone. This paper introduces a multi-sensor fusion steam generator secondary side inspection robot. Primary emphasis is on data fusion of multiple sensors, such as laser sensors, cameras, IMU, and wheel encoder. First of all, this paper integrates data from wheel encoder data and IMU data by using extended Kalman filtering (EKF), which decreases the drift error during the motion and enhances the robot positioning precision. Afterwards, we incorporate laser ranging sensors and camera picture data to enhance the overall spatial sensitivity of the robot through particle filtering algorithms. Experiments show that the robot works reliably and has high positioning accuracy.

Keywords: Multi-Sensor Fusion, Wall Climbing Robot, Nuclear Energy, Steam Generator

I. INTRODUCTION

Wall climbing robots as an integral component of the robotics field, Nishi [1] designed the world's first wall climbing robot. Generally, wall climbing robots can be classified according to the different ways of movement and adsorption, among which wheeled magnetic adsorption wall climbing robots are widely used [2]. SRI International PRAHLAD et al [3] firstly applied flexible electrostatic adhesion material to a tracked wall climbing robot. WU et al [4] designed a millimeter-scale wirelessly controlled soft robot driven by an external magnetic field that adhesion effect by a gecko-like material that can crawl on 3D biological tissue surfaces. CAO et al [5], National University of Singapore, developed an unconstrained soft robot with built-in power supply, which can achieve both turn and forward motion on a plane.

Since wall climbing robots are equipped with many sensors, many scholars have conducted intensive research on multi-

sensor fusion localization. T. Qin et al [6] proposed VINS-MONO with monocular camera and inertial measurement unit (IMU) fusion. C. Li et al [7] proposed a new architecture based on convolutional neural networks (RCNN) with fused IMU data for position estimation. Lina Li et al [8] proposed an algorithm for SLAM modified by integration of laser and vision. Yanjie Liu et al [9] extended the posenetLSTM convolutional neural network to involve vision and laser sensor information in the algorithm for robot localization. Wall climbing robots can replace humans to effectively complete various tasks in hazardous environments such as high altitudes [10-12]. Therefore, the research of wall climbing robots is of crucial value.

II. MULTIPLE SENSOR DATA FUSION METHODS

To address the problem of inaccurate positioning of the robot applying a single sensor in uncharted circumstances inside the steam generator, several integration schemes are proposed as shown in Figure 1.

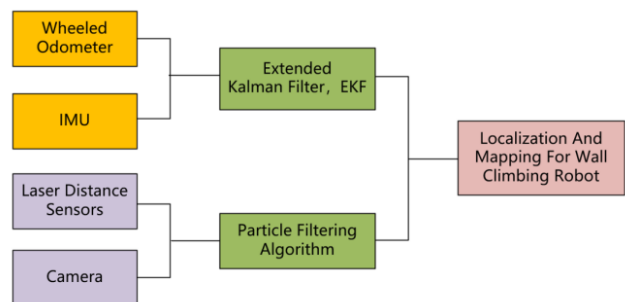


Figure 1. Flow chart of two fusion methods

A. Data conversion of IMU and wheeled odometer

The starting point where the robot starts to move after entering the hand hole is determined in Figure 2. The operating space coordinate system of the machine is based on the point O, and the center of mass of the whole vehicle is also the point O.

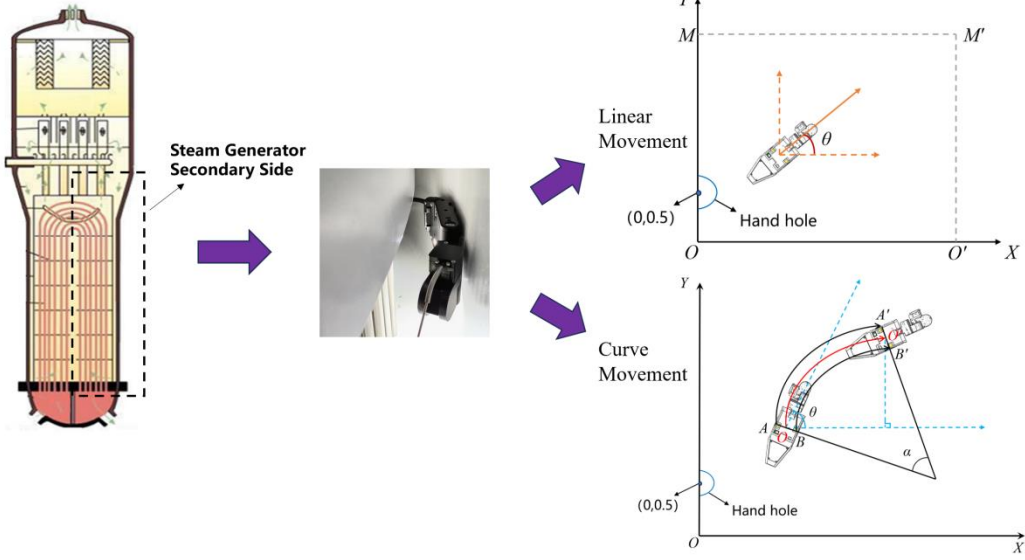


Figure 2. System coordinate establishment

The image frame rotation state at moment i is considered to be R_i and velocity state is V_i . We can compute the numerical integration over IMU to obtain the state quantity at moment j.

$$\begin{cases} R_j = R_i \prod_{m=i}^{j-1} \exp((\omega^m - b_G^m - \eta_G^m) \Delta t) \\ V_j = V_i + g^o \Delta t_{i,j} + \sum_{m=i}^{j-1} R_m (a^m - b_A^m - \eta_A^m) \end{cases} \quad (1)$$

The Δt is IMU sampling interval, ω is triaxial angular velocity and triaxial linear acceleration, η_A and η_G are Gaussian noise, and b_A and b_G are zero offsets.

EKF is used to solve nonlinear problems by linearizing the nonlinear system, specifically, EKF utilizes a first-order Taylor series expansion to approximate nonlinear function in order to transform the nonlinear problem into a linear one. Assuming that the state of the robot is $X_t = (x_t, y_t, \theta_t)^T$, the interval between data acquisition by the wheel encoder is Δt , ω_t is the angular velocity, v_x is the forward velocity, v_y is the lateral speed, and θ is the declination angle, then the robot's state transfer equation in continuous time can be given as:

$$X_t = \begin{bmatrix} \Delta t \cdot v_x \cos \theta_{t-1} + x_{t-1} \\ \Delta t \cdot v_y \sin \theta_{t-1} + y_{t-1} \\ \Delta t \cdot \omega_t + \theta_{t-1} \end{bmatrix} = X_{t-1} + \begin{bmatrix} \cos \theta_{t-1} & -\sin \theta_{t-1} & 0 \\ \sin \theta_{t-1} & \cos \theta_{t-1} & 0 \\ 0 & 0 & 1 \end{bmatrix} \begin{bmatrix} v_x \\ v_y \\ \omega_t \end{bmatrix} \Delta t \quad (2)$$

If the robot moves in continuous epochs, the equation of state for the prediction can be simplified owing to the presence of statistically defined noise S_t . The equations optimized are Equation (5), u is controlling incremental volume, J_{t-1} is the Jacobi matrix of X_{t-1} , with the corresponding covariance after simplification denoted as P_t :

$$\begin{aligned} \hat{X}' &= f(X_{t-1}, u_t) + S_t \\ P'_t &= J_{t-1} P_{t-1} J_{t-1}^T + S_t \end{aligned} \quad (3)$$

Therefore, the Kalman gain matrix K can be expressed as:

$$K_t = \frac{P_t^T H_t^T}{H_t^T P_t^T H_t^T + R_t} \quad (4)$$

The H_t is the measured Jacobi matrix of velocity at moment t, R_t is ordinarily distributed noise. Then we can obtain the observation equation X_t from IMU and write it as:

$$X''_t = \begin{bmatrix} x''_t \\ y''_t \\ \theta''_t \end{bmatrix} + S_t \quad (5)$$

The respective renewal equation and covariance equation are shown below:

$$\begin{aligned} \hat{X}_t &= (1 - K_t) \hat{X}'_t + K_t X''_t \\ P_t &= P'_t - K_t P'_t \end{aligned} \quad (6)$$

B. Fusion of visual information and laser data

In this paper, we use particle filtering to combine the data generated by laser ranging and the image message generated by camera. First, the camera and the laser distance sensor are united and calibrated to obtain the relative position connection between them. And each of sensors individually perceive situation where the robot is located and obtain corresponding data, we can fuse two kinds of information by particle filtering. Eventually, we use the integrated database for localization of the robot as input to SLAM. The steps to be taken are as follows:

- (1) Initialize particle collection:

Firstly, we should initialize a set of particles $(\chi_o^i)_{i=1}^N$, for N particles ($i = 1, 2, 3, \dots, N$), the weight of each particle is initialized as $w_0(\chi_o^i) = \frac{1}{n}$.

- (2) Sequential Importance Sampling:

The particle collection is used in the SIS algorithm to

represent the state probability distribution and the particles are weighted according to the observations to obtain an estimate of the system state. To obtain the observation z_k in this paper by image localization model, sampling N particles $x_k^i (i=1, 2, \dots, N)$, then the individual weight of each particle is calculated from the equation $q(x_k | x_{k-1}, z_k) = p(x_k | x_{k-1})$:

$$\omega(x_k^i) = \omega(x_{k-1}^i) \frac{p(z_k | x_k^i) p(z_k | x_{k-1}^i)}{q(z_k | x_{k-1}^i, z_k)} \quad (7)$$

The $\omega(x_k^i)$ is the weight of the time i-th sample at time k, $\omega(x_{k-1}^i)$ is the weight of the time i-th sample at time k-1. Eventually we denote the respective particle normalized weights as:

$$\omega_k^j = \frac{\omega_k^j}{\sum_{j=1}^N \omega_k^j} \quad (8)$$

(3) Sequential Importance Resampling:

The particle filter can use the valid sampling ratio Neff and

the default threshold N to evaluate the need for resampling. Neff is the criterion used to determine the diversity and effectiveness of the particle set. Neff expresses the number of particles with actual weights in the current particle set. The effect of resampling is to prevent the particle weights from degenerating. When the effective sampling scale Neff is under a certain threshold N, it is considered that the current particle set has to be resampled. If there is no need for resampling, the next step is taken.

(4) Output:

Export a collection of particles: $\{x_k^i, \omega_k^j\}_{i=1}^N$.

(5) Observation Updates:

We make the time $k = k + 1$, then read the additional data, evaluate the new observation and return to step (2).

III. EXPERIMENT AND RESULTS

For the purpose of proving the validity of the approach, we conducted different experiments in steam generator mock-up construction. The experimental platform erected is shown in Figure 3.

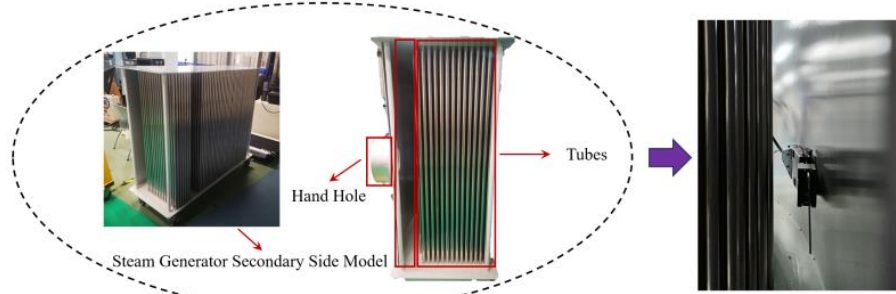


Figure 3. Steam generator mock-up construction

To verify the effectiveness of the scheme, we construct the experimental environment in a simulated body, and the experimental procedure is as follows. Firstly, we let the robot move a straight and curved trajectory from the starting point of the hand hole height without data fusion, and record the motion

trajectory of the vehicle body. Then the same experiment is performed again after data fusion, and the motion trajectory is recorded during the test. Finally, the vehicle motion data is compared between the pre-fusion and post-fusion.

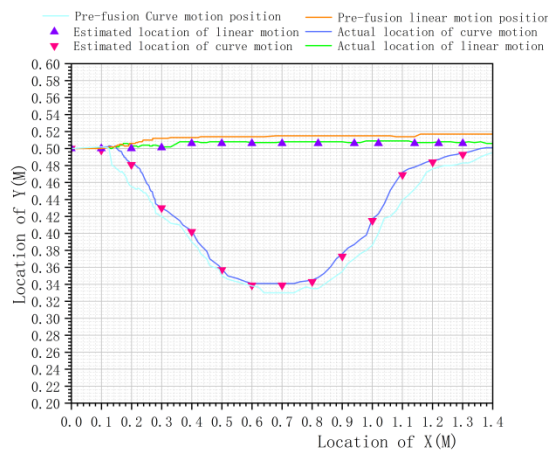


Figure 4. Straight and curved lines of motion

The results of the robot when it moves along a straight line are shown in Figure 4. The motion trajectories before and after data fusion are obviously different, and the mobile positioning after data fusion is closer to the predicted position. The maximum error after data fusion is no more than 1.2%, and this result is acceptable, thus we consider that the robot is accurately positioned in the mock-up body on the secondary side of the steam generator.

IV. CONCLUSIONS

Nuclear energy is regarded as one of the most vital energy sources on earth. The secondary side of the steam generator is the essential facility for nuclear power plants. Wall climbing robots have a prominent contribution in this field. The paper presents a multi-sensor fusion based wall-climbing robot. The experiment results demonstrate that the method of fusing wheel odometry and IMU data with EKF can optimize the accumulation of errors generated by the wheel in straight or curved motion, and the image data and laser data integrated by the particle filtering algorithm are better than the single sensor.

ACKNOWLEDGMENT

This work was partially supported by the National Natural Science Foundation of China under grant no. 62125307, in part by the NSFC Project under grant no. U2013212, and in part by the STS-HP-202201.

REFERENCES

- [1] Nishi A, Y Wakasugi and K Watanabe, Design of a robot capable of moving on a vertical wall. *Advanced Robotics*, 1986. 1(1): p. 33-45.
- [2] Fang Y, Wang S, Bi Q, et al. Design and Technical Development of Wall-Climbing Robots: A Review. *J Bionic Eng* 19, 877–901 (2022). <https://doi.org/10.1007/s42235-022-00189-x>
- [3] Prahlad H, Pehrline R, Stanford S, Marlow J and Kornbluh R, "Electroadhesive robots—wall climbing robots enabled by a novel, robust, and electrically controllable adhesion technology," 2008 IEEE International Conference on Robotics and Automation, Pasadena, CA, USA, 2008, pp. 3028-3033, doi: 10.1109/ROBOT.2008.4543670.
- [4] Wu Y, Dong X, Kim J, et al. Wireless soft millirobots for climbing three-dimensional surfaces in confined spaces [J]. *Science Advances*, 2022, 8(21): eabn3431.
- [5] Cao J, Qin L, Liu J, et al. Untethered soft robot capable of stable locomotion using soft electrostatic actuators[J]. *Extreme Mechanics Letters*, 2018, 21: 9-16.
- [6] T. Qin, P. Li and S. Shen, "VINS-Mono: A Robust and Versatile Monocular Visual-Inertial State Estimator," in *IEEE Transactions on Robotics*, vol. 34, no. 4, pp. 1004-1020, Aug. 2018, doi: 10.1109/TRO.2018.2853729.
- [7] Li C, Wang S, Zhuang Y, et al. Deep sensor fusion between 2D laser scanner and IMU for mobile robot localization[J]. *IEEE Sensors Journal*, 2019, 21(6): 8501-8509.
- [8] Li L, Yuan J, Sun H, et al. An SLAM Algorithm Based on Laser Radar and Vision Fusion with Loop Detection Optimization[C]//Journal of Physics: Conference Series. IOP Publishing, 2022, 2203(1): 012029.
- [9] Liu Y, Zhao C, Wei Y. A Robust Localization System Fusion Vision-CNN Relocalization and Progressive Scan Matching for Indoor Mobile Robots[J]. *Applied Sciences*, 2022, 12(6): 3007.
- [10] Iqbal J, Tahir A M, ul Islam R. Robotics for nuclear power plants—challenges and future perspectives[C]//2012 2nd international conference on applied robotics for the power industry (CARPI). IEEE, 2012: 151-156.
- [11] J. Zhou, J. Fu, R. Pan, G. Tian and Y. Li, "Structural design and research of underwater inspection robot for nuclear power plant," 2022 IEEE Conference on Telecommunications, Optics and Computer Science (TOCS), Dalian, China, 2022, pp. 1102-1107, doi: 10.1109/TOCS56154.2022.10015995.
- [12] Petereit J, Beyerer J, Asfour T, et al. ROBDEKON: Robotic systems for decontamination in hazardous environments[C]//2019 IEEE International Symposium on Safety, Security, and Rescue Robotics (SSRR). IEEE, 2019: 249-255.